Thermally Induced Fibrillar Aggregation of Hen Egg White Lysozyme

Luben N. Arnaudov and Renko de Vries
Laboratory of Physical Chemistry and Colloid Science, Wageningen University, Wageningen, The Netherlands

ABSTRACT We study the effect of pH and temperature on fibril formation from hen egg white lysozyme. Fibril formation is promoted by low pH and temperatures close to the midpoint temperature for protein unfolding (detected using far-ultraviolet circular dichroism). At the optimal conditions for fibril formation (pH 2.0, $T = 57°C$), on-line static light-scattering shows the formation of fibrils after a concentration-independent lag time of ~48 h. Nucleation presumably involves a change in the conformation of individual lysozyme molecules. Indeed, long-term circular dichroism measurements at pH 2.0, $T = 57°C$ show a marked change of the secondary structure of lysozyme molecules after ~48 h of heating. From atomic force microscopy we find that most of the fibrils have a thickness of ~4 nm. These fibrils have a coiled structure with a periodicity of ~30 nm and show characteristic defects after every four or five turns.

INTRODUCTION

Linear structures formed by proteins such as actin and tubulin are reversible and highly dynamic. Misfolded or partly unfolded globular proteins also often form linear structures but these fibrillar protein aggregates usually form slowly and are essentially irreversible. A case in point are the amyloidoses, such as Alzheimer's disease, Creutzfeld-Jacob disease, prion disease, etc. These are associated with deposition of fibrillar protein aggregates in various organs (Sunde and Blake, 1998). For most of these proteins conditions have also been found under which they form fibrillar aggregates in vitro (Chamberlain et al., 2000; Jimenez et al., 2001, 2002; Zurdo et al., 2001).

A very different example of fibrillar protein aggregates is the formation of transparent heat-set gels by various food proteins (Langton and Hermansson, 1992; Kavanagh et al., 2000; Koike et al., 1996). Such gels often form under conditions of strong electrostatic repulsion (pH far away form the protein isoelectric point and low ionic strength). Electron microscopy (Kavanagh et al., 2000; Aymard et al., 1999) and atomic force microscopy (Ikeda and Morris, 2002) have revealed that these transparent gels also consist of fibrillar protein aggregates. Heat-set fibrillar gels have been reported for ovalbumin (Nemoto et al., 1993), β-lactoglobulin (Kavanagh et al., 2000), and bovine serum albumin (Tani et al., 1995), to name but a few food proteins.

In a previous work (Arnaudov et al., 2003), mainly motivated by food applications, we investigated fibril formation of β-lactoglobulin (β-lg) at a temperature of 80°C, pH 2, and low ionic strength. On-line proton NMR spectroscopy and static and dynamic light-scattering were used to characterize the aggregation process. We found that fibrils start forming immediately after the heating has started, without any detectable lag time. Fibril formation is a multistep process: freshly formed fibrils still disintegrate upon slow cooling, but aged fibrils do not. Below an initial protein concentration of ~2.5 wt % fibril formation is no longer the dominant process. Instead, at low concentrations, most protein molecules go to an unfolded or partially folded state from which fibrils can no longer be formed.

It is not exactly clear to what extent fibril formation is mechanistically similar for different proteins under similar circumstances. Although some authors have called the fibrils such as those formed by β-lactoglobulin ''amyloid fibrils'' (Gosal et al., 2002; Sagis et al., 2004), no detailed comparison has been made, yet. Therefore, we here continue our studies of heat-induced fibril formation by studying fibrillar aggregation of hen egg white lysozyme (HEWL) under conditions (temperature of 57°C, pH 2–4, and low ionic strength) similar to those used in our previous study of β-lactoglobulin.

HEWL has been recently found to form amyloid fibrils in vitro (Krebs et al., 2000; Goda et al., 2000; Cao et al., 2004). It is also one of the best characterized and most studied of all proteins. Its folding-unfolding has been studied in detail (Redfield and Dobson, 1988; Radford et al., 1992; Itzhaki et al., 1994; Dobson et al., 1994) and unfolding intermediates have been found. It is also an important food protein.

Furthermore, HEWL is homologous to human lysozyme, which is one of the proteins that cause an amyloid disease upon mutation (Booth et al., 1997; Pepys et al., 1993) and for which aggregation is also observed in vitro (Morozova-Roche et al., 2000). The formation of amyloid aggregates in vitro by wild-type and point-mutated human lysozyme has been studied by Morozova-Roche et al. (2000). Amyloid fibril formation was observed upon incubation of the wild-type and the variant human lysozymes at conditions in which partially folded intermediates are highly populated. Seeding experiments proved that the fibril formation was greatly

Submitted July 1, 2004, and accepted for publication October 4, 2004.

Address reprint requests to Renko de Vries, Laboratory of Physical Chemistry and Colloid Science, Wageningen University, PO Box 8038, Wageningen 6700 EK, The Netherlands. Tel.: 31-317-484561; E-mail: renko.devries@wur.nl.

0006-3495/05/01/515/12 $2.00

doi: 10.1529/biophysj.104.048819

influenced by the presence of the seeds. Amyloid aggregates have also been found to form from equine lysozyme (Malisauskas et al., 2003). Short fibrils and rings were observed by atomic force microscopy (AFM), which was used as a basic monitoring technique.

The only study of the formation of amyloid fibrils by wild-type HEWL induced by heat treatment alone is that of Krebs et al. (2000). Fibrils were formed from aqueous solutions at pH 2.0 by incubation at 37°C after a brief heat shock at 100°C followed by freezing in liquid nitrogen, or by simple incubation at 65°C. Fibrils were also formed at pH 7.4 in solution containing 30% 2,2,2-trifluorethanol by incubation either at 37°C or at 65°C. Other studies of HEWL amyloid fibril formation invariably involve denaturing agents such as ethanol (Goda et al., 2000; Yonezawa et al., 2002; Tanaka et al., 2001) or even full reduction of the protein (Cao et al., 2004). No study has yet been done on fibril formation by HEWL using the simplest procedure of heating an aqueous solution at a constant temperature. Also there are practically no data about the kinetics of the fibril formation from HEWL. For human lysozyme, Morozova-Roche et al. (2000) studied the fibrillar aggregation induced by heating at 57°C at pH 2. Following these authors, we here study the fibrillar aggregation of HEWL induced by heating at 57°C at pH 2. We also explore the effects of increasing the pH (up to 4) and temperature (up to 80°C). The kinetics of aggregation is studied by on-line static light scattering (SLS). The intensity of the scattered light is particularly sensitive to the size of the scattering objects, which makes the method very useful in detecting the onset of the aggregation. The type of the aggregates and their morphology are studied in detail by AFM. The effect of the temperature and the heating time on the secondary structure of HEWL at different pH values is studied by circular dichroism (CD). Prolonged heating at pH 2 may cause protein hydrolysis, which may or may not influence the course of the aggregation process. Therefore we also perform tris-tricine sodium dodecyl sulfate polyacrylamide gel electrophoresis (SDS-PAGE) on the heat-treated protein solutions.

MATERIALS AND METHODS

Materials

Hen egg white lysozyme was obtained from SIGMA (6× crystallized and lyophilized, L-6876, Lot 51K7028). All solutions were prepared with deionized water (Barnstead) and contained 200 ppm NaN_3 to prevent bacterial growth. Before use a concentrated solution of HEWL at pH 4.0 was extensively dialyzed against the solvent (aqueous solution of HCl at pH 4.0). The solutions used in all the experiments were prepared by dilution from the dialyzed one. The pH was adjusted by addition of small amounts of 1 M HCl (Merck, Darmstadt, Germany). The ionic strength of the protein solutions at pH higher than 2.0 was adjusted to 13 mM by addition of NaCl (Merck). Care was taken to minimize dust. Glassware was cleaned with chromic acid, rinsed with plenty of deionized water and dried in a clean environment. The protein solutions were filtered through 0.1 μm Acrodisc syringe filters (Gelman Laboratory) into the glass tubes in which the experiments were subsequently carried out. The protein concentrations were determined by a Hitachi U-2010 spectrophotometer at $\lambda = 280$ nm, using an extinction coefficient of 2.65 L g^{-1} cm^{-1}.

Methods

Static light scattering

SLS data were obtained at a scattering angle of 90° using an ALV/SLS/DLS-5000 light-scattering apparatus (ALV, Langen, Germany), equipped with an argon ion laser (LEXEL, Palo Alto, CA) operating at a wavelength of 514.5 nm. Two types of experiments were carried out. In the first one the sample holder of the instrument was preheated to the desired temperature (57°C, 60°C, 65°C, or 80°C), the sample was introduced in the sample holder, and the intensity of the scattered light was recorded continuously for as long as 2 days. In the second type of experiment samples of each protein concentration were introduced in a thermostatic bath preheated at the desired temperature, the sample holder of the light scattering apparatus was preheated to the same temperature, and at regular time intervals the samples were quickly replaced from the bath to the light-scattering equipment and the intensity of the scattered light was measured. The intensity of the scattered light was calibrated by the intensity of the scattered light from pure toluene measured before each series of experiments at 25°C. Before heating, the presence of only monomeric protein in the samples was established by dynamic light scattering (scattering angle 90°, temperature 25°C) for each sample.

Atomic force microscopy

Tapping mode AFM was carried out using a Nanoscope III, multimode scanning force microscope (Digital Instruments, Santa Barbara, CA). Observations were performed on dry samples in air prepared as follows. Clean silicon plates were used as substrates. The plates were cleaned first in pure ethanol by ultrasound, then rinsed with pure ethanol and dried with pure and dry nitrogen. The dry silicon plates were subsequently subjected to plasma cleaning. After the plasma cleaning the silicon plates were dipped into test protein solutions for 1 h, taken out and dried immediately using pure and dry nitrogen. The test protein solutions were prepared by taking aliquots at regular time intervals from HEWL solutions kept in tightly closed glass tubes in a preheated bath at the desired temperature, quenching the aliquots in ice-cold water and diluting them to a final protein concentration of 0.1 wt %.

Circular dichroism

Circular dichroism spectra were recorded by using a Jasco J-715 spectropolarimeter (Jasco, Tokyo, Japan). Far-ultraviolet (UV) (185–260 nm) spectra were recorded in 0.01 cm path length cell (Hellma, Muellheim/Baden, Germany) using a step size of 0.5 nm, bandwidth of 1 nm, and scan rate of 50 nm/min. Each protein spectrum was obtained by averaging 10 scans and corrected by subtracting the solvent spectrum. The temperature was varied between 25°C and 90°C by means of a computer-controlled Peltier device (PTC-348WI, Jasco). The temperature scan was carried out on fresh protein solutions with concentration of 0.2 wt %. At every temperature the sample was allowed to equilibrate for 5 min before the wavelength scan series was started. Spectra were also recorded at 25°C from quenched samples of already heated protein with concentrations of 0.1 wt %. The quenched samples were obtained by the procedure described in the previous section.

SDS-PAGE

Gel electrophoresis was performed under nonreducing conditions using commercial SDS/polyacrylamide gels (16.5% Tris-Tricine precast gels,

BioRad, Hercules, CA). Reference polypeptide mixture was purchased from BioRad. Coomassie brilliant blue R250 (Sigma, St. Louis, MO) was used for staining.

RESULTS

Light scattering

The intensity of the scattered light is extremely sensitive to the presence of large objects such as protein aggregates. We use light scattering to detect the onset of aggregation. Fig. 1 shows the intensity of the scattered light as a function of the heating time at 57°C for samples of 2.0 wt % HEWL at three different pH values (2.0, *circles*; 3.0, *squares*; and 4.0, *triangles*). The dependence of the scattered intensity on the heating time, in the cases when aggregation occurs (pH 2.0 and 3.0), is very characteristic; the intensity stays constant for a long time and then rapidly increases. At pH 2.0 the aggregation starts after almost 2 days of heating. At pH 3.0 the aggregation starts after >10 days of heating. The scattered intensity for HEWL solution at pH 4.0 stays virtually constant during 42 days (data shown until day 20), thus showing no signs of aggregation.

To study the kinetics of fibril formation from HEWL in more detail, light-scattering experiments with different initial protein concentration are carried out at pH 2.0, 57°C (see Methods). We observed that there was a large spread from sample to sample, both in the time at which the intensity starts to increase and in the rate of increase of the scattered intensity. To obtain reliable data the scattered intensity was averaged over 10 samples for each concentration. Fig. 2 *a* shows the averaged data for increasing initial concentrations of lysozyme (1.0 wt %, *circles*; 2.0 wt %, *squares*; and 3.0 wt %, *triangles*). Fig. 2 *b* shows the time at which the aggregation starts, calculated from the data plotted in Fig. 2 *a*.

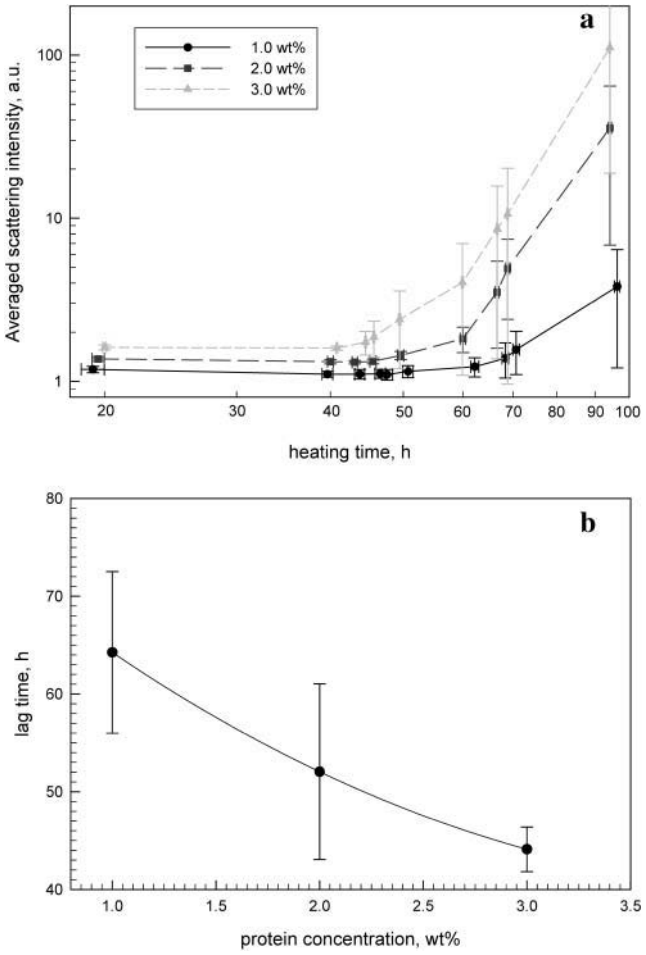

FIGURE 2 (*a*) Intensity of the scattered light with heating time for three sample series with three different concentrations of HEWL: 1.0 wt % (*circles*), 2.0 wt % (*squares*), and 3.0 wt % (*triangles*), as determined by LS. (*b*) Lag time as a function of protein concentration as estimated from the data presented in *a*.

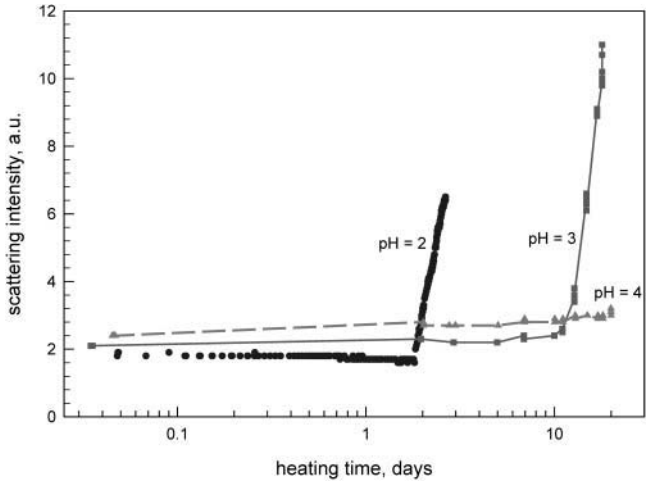

FIGURE 1 Intensity of the scattered light as a function of the heating time for 2.0 wt % HEWL at pH 2.0 (*circles*), pH 3.0 (*squares*), and pH 4.0 (*triangles*) heated at 57°C, as determined by SLS at a scattering angle of 90°.

As one can see the lag time plotted in Fig. 2 *b* hardly depends on the initial protein concentration. This suggests that the aggregation process involves some monomolecular nucleation step, i.e., a slow change in the conformation of the protein molecules precedes the aggregation.

We also explored the aggregation process at higher temperatures. Light-scattering experiments with HEWL solutions at pH 2.0, 3.0, and 4.0 were performed at 60°C, 65°C, and 80°C. The results obtained upon heating at 60°C and 65°C do not differ from those obtained at 57°C. Upon heating solutions at pH 2.0, 3.0, and 4.0 at 80°C, the intensity of the scattered light starts to increase immediately after the samples are placed in the preheated sample holder and the temperature is equilibrated, i.e., the aggregation starts immediately. At pH 2.0, fibrillar aggregates accompanied by spherical aggregates are formed (see Atomic force microscopy). At pH 3.0 and 4.0 only spherical aggregates are formed (see Atomic force microscopy). The effective

hydrodynamic radius of the spherical aggregates formed after 6 days of heating at 80°C at pH 4.0 (measured using dynamic light scattering) is $R_H = 24$ nm.

Atomic force microscopy

AFM is used both to confirm the presence of fibrillar aggregates in the HEWL samples at pH between 2.0 and 4.0, heated for different times at temperatures between 57°C and 80°C, and to study the fibril morphology in as much detail as possible.

Fig. 3 shows tapping mode AFM height images of fibrils formed from HEWL solutions at pH 2.0 heated at 57°C, 60°C, and 80°C. Fibrils are formed in all cases, though at 80°C a considerable amount of spherical aggregates are formed, too. The fibrils formed are very long, thin, and straight.

For HEWL solutions at pH 2.0 heated at 57°C the average fibril length is >5 μm and the longest fibril observed was 16 μm. Mostly thick and some thin fibrils are observed (see Fig. 3, *c* and *d*). The thick fibrils consist of shorter rodlike subunits, as shown in detail in Fig. 4, *a* and *b*. Fig. 4, *a* and *b*, are identical tapping mode AFM height images of HEWL fibrils, as Fig. 4 *a* shows the original image and Fig. 4 *b* shows the same image superimposed with marks of the visible boundaries of the rodlike subunits. In the inset in Fig. 4 *b* a blow-up of one of the boundaries between such subunits (marked by a *white arrow*) is shown. In Fig. 3, *c* and *d*, one can see examples of bending occurring at boundaries between different subunits. The subunits themselves remain straight. With increasing initial protein concentration the number of fibrils observed increases and they tend to form bundles (Fig. 3 *d*).

A histogram of the distribution of the fibril thicknesses is shown in Fig. 5 *a*. A small population (~10%) of thin fibrils can be observed in Fig. 5 *a* with an average thickness of 2.5 ± 0.3 nm. Most fibrils are thick and have an average diameter of 4.0 ± 0.7 nm.

In Fig. 5 *b*, a histogram of the distribution of the fibril subunit length is plotted. The subunit length shows a bimodal distribution with average lengths of 124 ± 9 nm and 157 ± 11 nm, respectively. As both lengths are multiples of ~30 nm and the difference between the peaks is also ~30 nm one may suspect the presence of a length scale in the fibrils smaller than the subunit length and equal to ~30 nm.

To validate the latter assumption we carried out a set of experiments with super sharp tapping mode AFM tips with

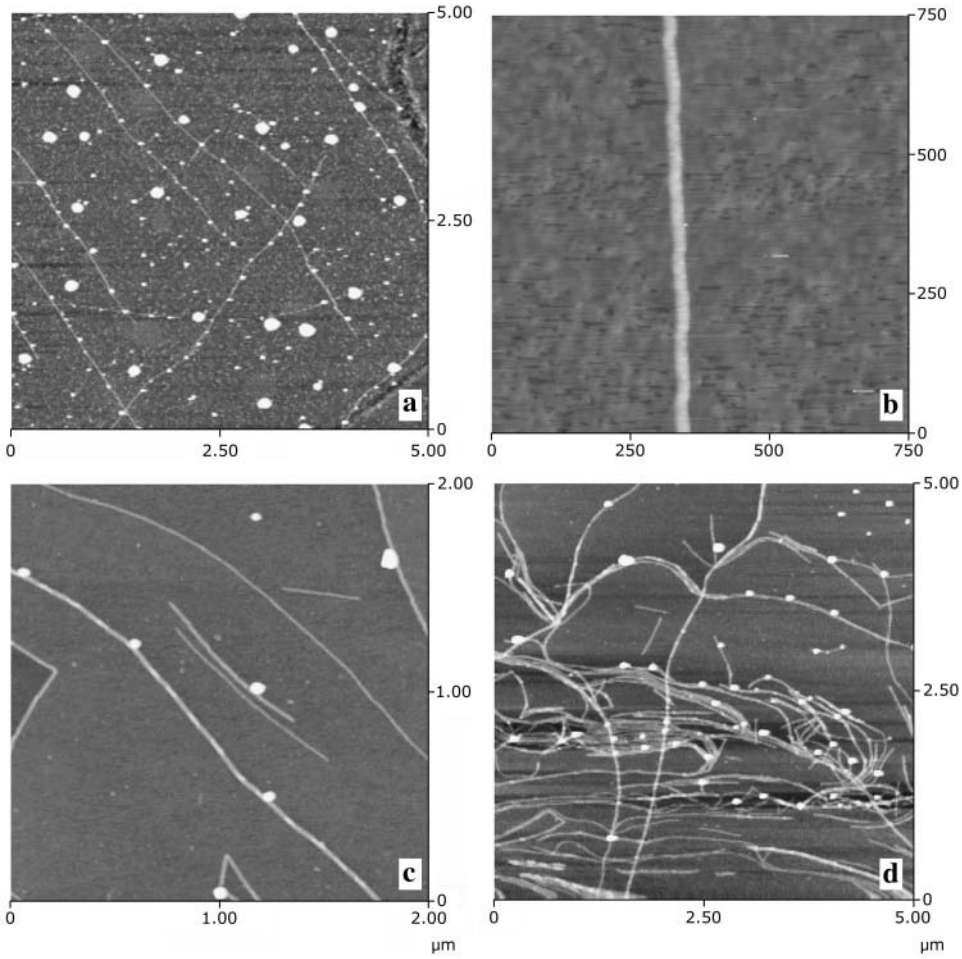

FIGURE 3 Tapping mode AFM height images of fibrils formed from lysozyme solutions at pH 2.0: (*a*) 1.0 wt %, 4 days at 80°C; (*b*) 1.0 wt %, 6 days at 60°C; (*c*) 2.0 wt %, 69 h at 57°C; (*d*) 3.4 wt %, 69 h at 57°C.

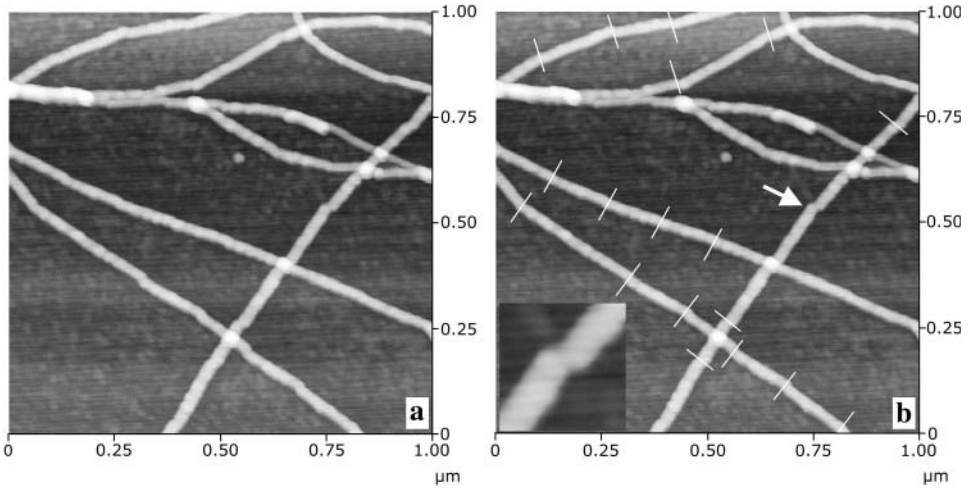

FIGURE 4 (*a*) Tapping mode AFM height images of fibrils formed from 2.0 wt % lysozyme at pH 2.0, heated for 13 days at 57°C; (*b*) The same as in *a* with marks on the visible subunits boundaries (*white lines*). The inset shows a blow-up of the connection between two subunits marked by an arrow.

a curvature at the tip of ~2 nm (Nanosensors, Wetzlar-Blankenfeld, Germany). The standard tapping mode AFM tips have a curvature at the tip of ~10 nm, which makes the observation of lateral details of the order of 20 nm practically impossible because of the sample-tip convolution effects. Fig. 6 shows four consecutive tapping mode AFM height images of a fibril formed upon heating of HEWL, pH 2.0, at 57°C. Indeed one can identify a coiled substructure of the fibril with a periodicity of ~30 nm (Fig. 6, *c* and *d*). The substructure observed by us in this preliminary experiment will be studied in more detail in the near future.

HEWL solutions at pH 3.0 and 4.0 do not form fibrillar aggregates when heated at 80°C within a week. Instead, spherical aggregates are observed (data not shown). HEWL does form fibrillar aggregates at pH 3.0 upon heating at 57°C. The first aggregates are observed after 11 days of heating. No aggregates whatsoever could be detected for HEWL solutions at pH 4.0 heated at 57°C for as long as 42 days. In Fig. 7 tapping mode AFM height images of samples taken from 2.0 wt % HEWL solutions heated at 57°C for 13 days at pH 2.0 (Fig. 7 *a*), 3.0 (Fig. 7 *b*), and 4.0 (Fig. 7 *c*) are shown for comparison. The fibrils formed at pH 3.0 are long and thin, similar to the ones formed at pH 2.0 but more flexible. Only lysozyme monomers can be seen for pH 4.0 (Fig. 7 *c*).

Circular dichroism

The experimental results from light scattering and AFM indicate a pronounced pH dependence of the aggregation process, which is most likely related to the dependence of the protein stability on pH. This issue was investigated using far-UV circular dichroism. CD experiments were carried out on samples at pH 2.0, 3.0, and 4.0, and also on samples at pH 2.0 quenched after different periods of heating ranging from 24 h to 11 days.

Fig. 8 *a* shows CD spectra of HEWL at pH 2.0 measured at temperatures from 25 to 85°C at 5°C intervals. The spectra from 25°C to 45°C practically coincide with the native one. A major change in the spectrum occurs between 50°C and 60°C as the ellipticity between 208 and 230 nm increases and the minimum at 208 nm moves to a lower wavelength with increasing temperature, as the final value reached at 85°C is 202 nm. Above 60°C all spectra practically coincide. After

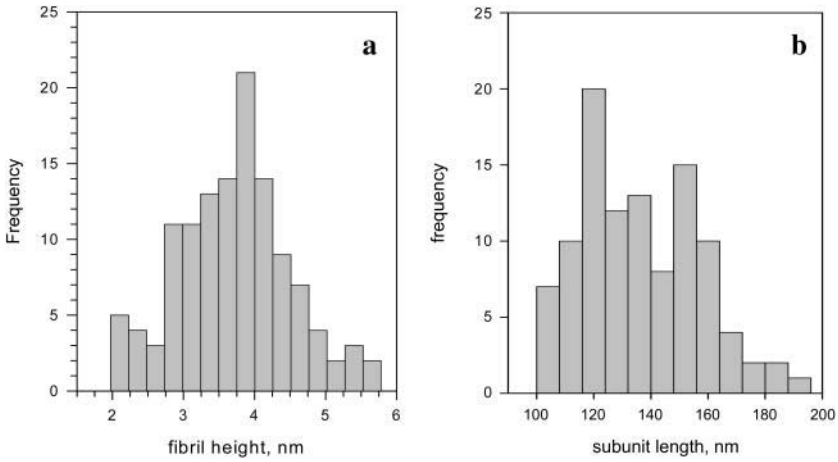

FIGURE 5 (*a*) Histogram of the height of HEWL fibrils formed at pH 2.0, 57°C; (*b*) Histogram of the subunit length of HEWL fibrils formed at pH 2.0, 57°C.

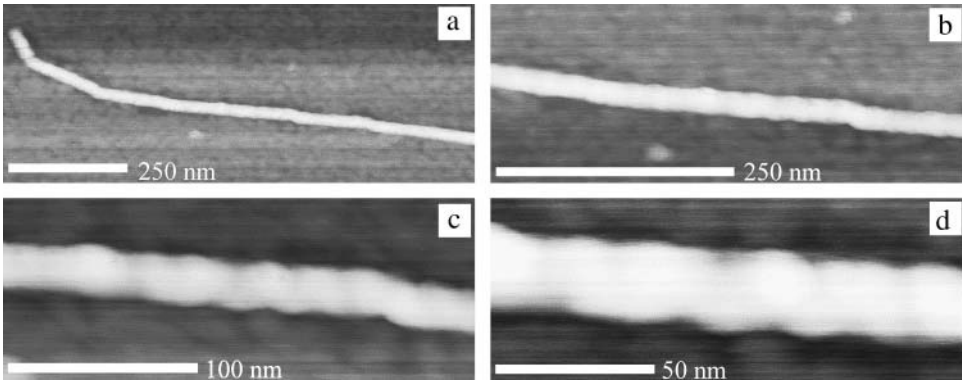

FIGURE 6 Consecutive tapping mode AFM height images of a fibril from solution of 2.0 wt % HEWL at pH 2.0 heated for 13 days at 57°C. The scale of each individual image is indicated by a white bar.

the T ramp the sample was cooled back to 25°C. The spectrum of that sample did not fully coincide with the initial spectrum measured at 25°C (data not shown), i.e., the unfolding transition induced by heating is not fully reversible.

In Fig. 8 *b*, spectra of HEWL at pH 3.0 measured at temperatures from 25°C to 85°C at 5°C intervals are plotted. One can see that the spectra resemble the native one from 25°C to 65°C. A change in the spectrum similar to that observed at pH 2.0 is observed in Fig. 8 *b* between 65°C and 80°C. The spectra above 80°C practically coincide.

In Fig. 8 *c* spectra of HEWL at pH 4.0 measured at temperatures from 25°C to 90°C at 5°C intervals are plotted. In this case the spectra resemble the native one up to 70°C. The change in the spectrum occurs between 70°C and 85°C. Above 85°C the spectra coincide.

For all pH values studied, an isodichroic point is observed at 204 nm, suggesting that unfolding is a two-state cooperative process (Fändrich et al., 2003). To determine midpoint temperatures for the unfolding transition, we use the ellipticity at 222 nm (Yang et al., 1994; Sasahara et al., 2000). A plot of the molecular residue ellipticity at 222 nm of HEWL solutions at pH 2.0, 3.0, and 4.0 as a function of temperature is given in Fig. 9. The data are fitted by sigmoid curves. Midpoint temperatures of the transition obtained in this way are 54.8 ± 0.2°C for pH 2.0, 72.7 ± 0.7°C for pH 3.0, and 78.0 ± 0.5°C for pH 4.0. Transition temperatures decrease very rapidly at low pH, indicating a much less stable protein molecule at pH 2.0.

We have also used CD to quantify changes in secondary structure upon prolonged heating of HEWL at 57°C, pH 2.0. Fig. 10 *a* shows molecular residue ellipticities of a continuously heated HEWL sample measured after 5 min, 20 h, 26 h, 44 h, 50 h, and 65 h, respectively. The CD spectrum of the protein keeps changing with heating time. The ellipticity between 190 and 240 nm decreases, indicating continuous structural changes in the protein molecule with heating time. Generally, the decrease of the ellipticity between 208 and 230 nm corresponds to an increase in the amount of α-helix in the secondary structure of the protein. Also, a jump in the ellipticity is observed between 44 and 50 h of heating. This is shown in Fig. 10 *b*, where the molecular residue ellipticity at 222 nm during the continuous heating of the HEWL sample is plotted. From a sigmoid fit of the experimental data we found that the jump occurred at a heating time of 48 h (see Fig. 10 *b*). This time coincides with the lag time after which the aggregation is detected by light scattering. One possible scenario is a process in which the partly destabilized lysozyme, which is still not capable of forming fibrils, undergoes a structural change after which it is susceptible to amyloid aggregation.

Finally, we separated the fibrils from the monomers by filtration and measured their spectra separately. Fig. 11 shows the molecular residue ellipticities of a sample of HEWL at pH 2.0 quenched after 11 days of heating at 57°C. The spectra of the monomers and fibrils from the same sample are plotted together with the spectrum of the protein quenched after 24 h of heating at 57°C for the sake of comparison. The spectrum of the separated monomers (*FF*,

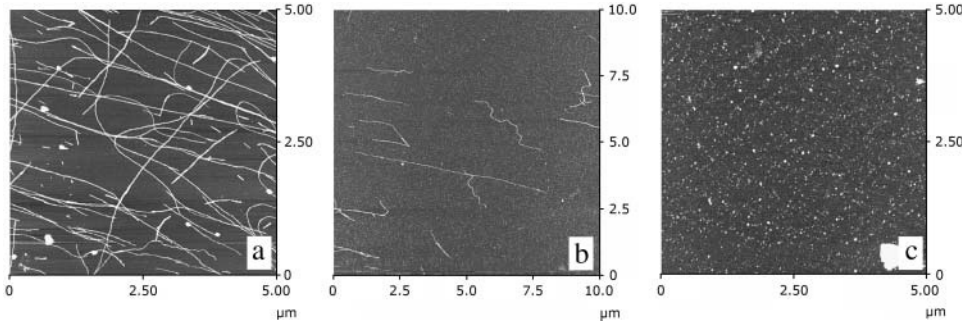

FIGURE 7 Tapping mode AFM height images of 2.0 wt % HEWL heated for 13 days at 57°C: (*a*) pH 2.0; (*b*) pH 3.0; (*c*) pH 4.0.

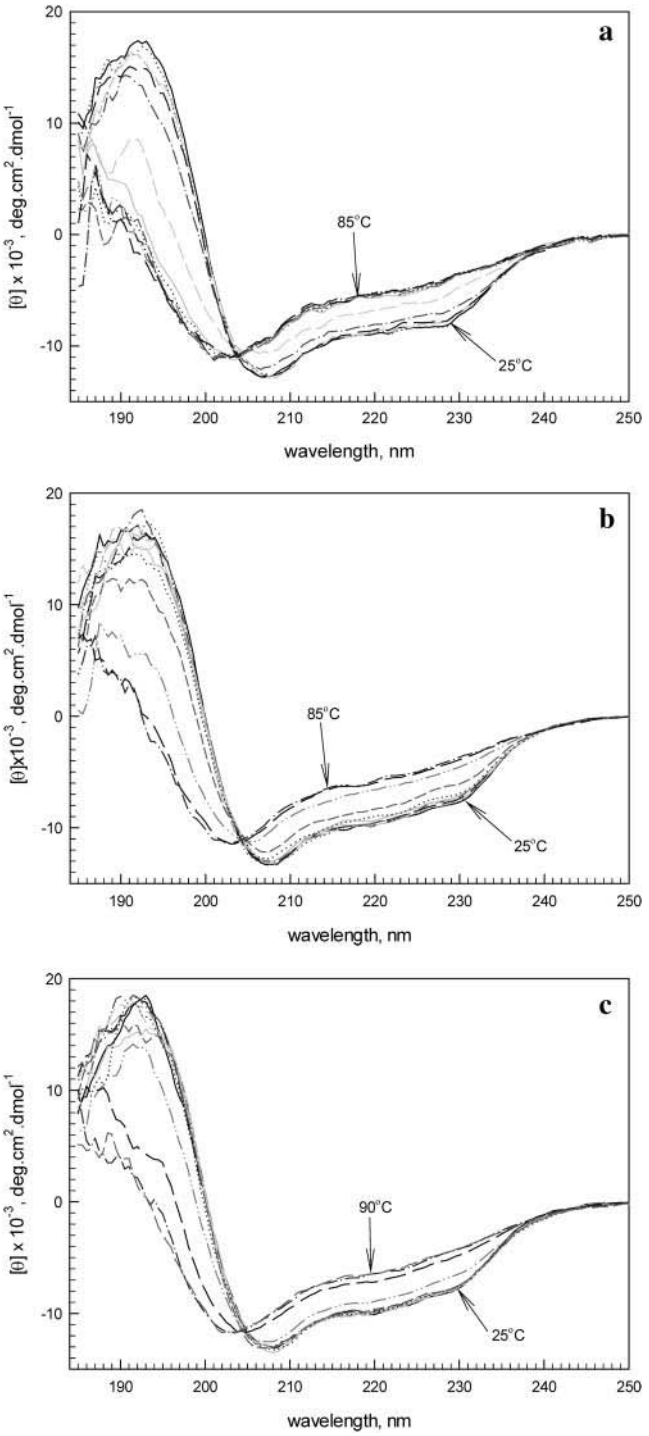

FIGURE 8 (*a*) Molecular residue ellipticity of HEWL at pH 2.0 for a range of temperatures between 25°C and 85°C. (*b*) Molecular residue ellipticity of HEWL at pH 3.0 for a range of temperatures between 25°C and 85°C. (*c*) Molecular residue ellipticity of HEWL at pH 4.0 for a range of temperatures between 25°C and 90°C.

filtered fraction) is similar to that of the whole sample. Both spectra show features typical of spectra of largely unfolded proteins, i.e., almost no characteristic features except the minima at ~202 nm, which is typical for a random-coil

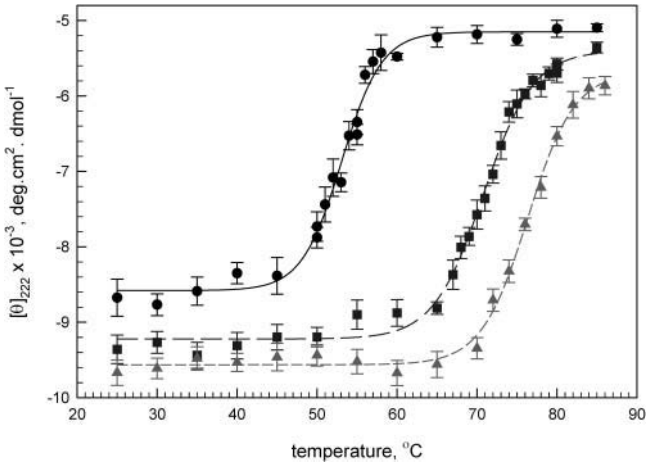

FIGURE 9 Molecular residue ellipticities of HEWL at 222 nm for three different pH values versus temperature: pH 2.0 (*circles*), pH 3.0 (*squares*), and pH 4.0 (*triangles*). The lines represent the best fit with a sigmoid curve. The midpoints of the transition between the two states are 54.8 ± 0.2°C for pH 2.0, 72.7 ± 0.7°C for pH 3.0, and 78.0 ± 0.5°C for pH 4.0.

protein. The spectrum of the fibrils (*OLA*, only large aggregates) has a similar minimum around 200 nm, but a small minimum at ~218 nm can be observed that may be due to the presence of β-sheet.

SDS-PAGE

Prolonged heating at low pH may cause protein hydrolysis that may or may not influence the course of the aggregation process. Nonreducing SDS-PAGE was used to determine the extent of hydrolysis. Fig. 12 shows the results of gel electrophoresis. Lanes 1–3 correspond to native HEWL at natural pH, pH 2.0, and pH 3.0, respectively. Lanes 4, 5, 7, and 8 correspond to HEWL at pH 2.0 quenched after 24 h, 72 h, 168 h, and 11 days of heating at 57°C. Lane 6 corresponds to a polypeptide molecular weight standard. Lane 9 corresponds to HEWL at pH 3.0 quenched after 38 days of heating. Lanes 10 and 11 correspond to HEWL at pH 2.0, quenched after 11 days of heating subjected to separation: in lane 10 is a filtered fraction of HEWL (only monomers), and in lane 11 only large (fibrillar) aggregates.

No bands corresponding to large protein aggregates were observed. This implies that fibril formation does not involve covalent bonds (e.g., disulfide bridges), but only physical bonds, which are broken down by heating in the presence of SDS.

Gradual fragmentation is indeed observed, but only at pH 2.0 and for very long times of heating at 57°C (*lanes 4*, *5*, *7*, and *8*). The protein that is not heated (*lanes 1–3*) is intact as only one bright line can be seen for each of the three samples. Although the line of the monomeric protein is thick and bright even for the sample heated for 11 days (*lane 8*), one can see one or more lines corresponding to lower-molecular

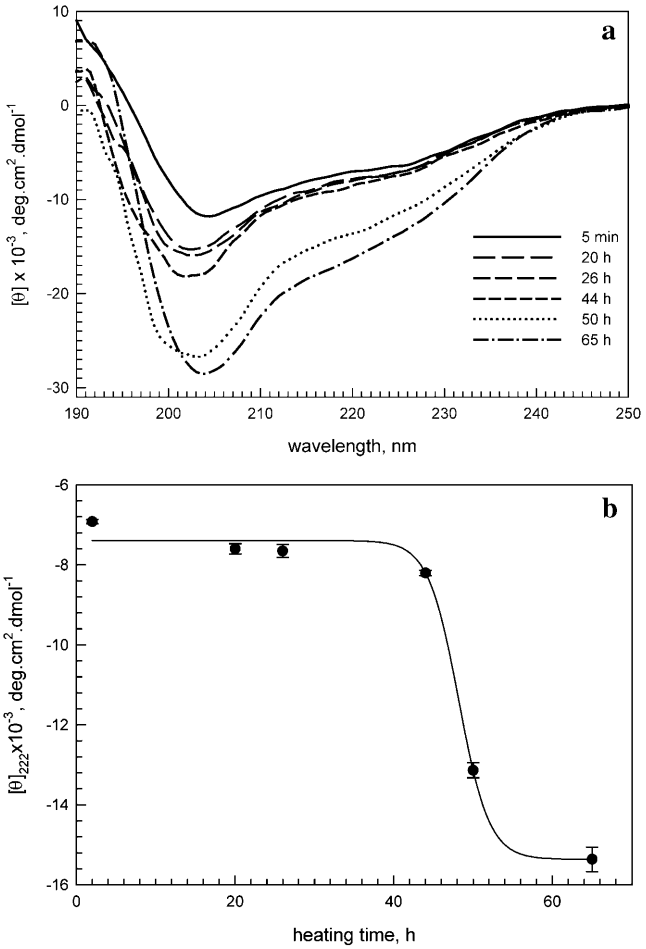

FIGURE 10 (*a*) Molecular residue ellipticities of continuously heated at 57°C HEWL sample at pH 2.0 measured after, 5 min, 26 h, 44 h, 50 h, and 65 h. (*b*) Molecular residue ellipticity at 222 nm during the continuous heating at 57°C of a HEWL sample at pH 2.0.

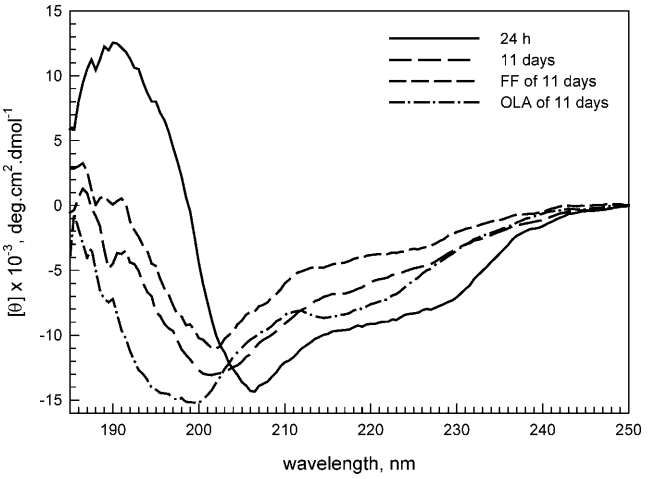

FIGURE 11 Molecular residue ellipticities of HEWL at pH 2.0, quenched after being heated at 57°C for 24 h (*solid line*) and 11 days (*long-dashed*, *short-dashed*, and *dot-dashed lines*). *FF*, filtered fraction: a fraction that contains only monomeric lysozyme; *OLA*, only large aggregates: a fraction that contains only fibrils obtained by washing the monomers off.

weight species appearing below the native one. The process is slow: for the sample heated for 24 h (*lane 4*) a line corresponding to ~10-kDa fragments is barely visible. The brightness of this line increases with heating time (*lanes 5*, *7*, and *8*). One can also see additional lines for the samples heated for 7 and 11 days, corresponding to fragments with molecular weights <6,500.

Samples heated for 11 days at 57°C, pH 2.0, were again separated into monomers and fibrils using filtration. Lanes 10 and 11 correspond to low-molecular weight species and long aggregates, respectively, after being separated from a sample of HEWL at pH 2.0 heated for 11 days. The lines in lane 11 practically coincide with the lines in lane 8—an identical sample not subjected to separation of the low-molecular weight species and the fibrils. The lines in lane 10 are similar to those in lanes 8 and 11 but less pronounced due to the smaller amount of protein applied to the gel in that lane. Clearly the fibrils do not exclusively consist of either full-length protein or protein fragments.

Finally, for pH 3.0 quenched after 38 days of heating at 57°C (*lane 9*), no hydrolysis is observed in SDS-PAGE, which indicates that hydrolysis is not a prerequisite for fibril formation.

DISCUSSION

It has been shown by a number of authors that lysozymes form amyloid aggregates under a variety of denaturing conditions (Morozova-Roche et al., 2000; Malisauskas et al., 2003; Krebs et al., 2000). Obviously the protein molecule

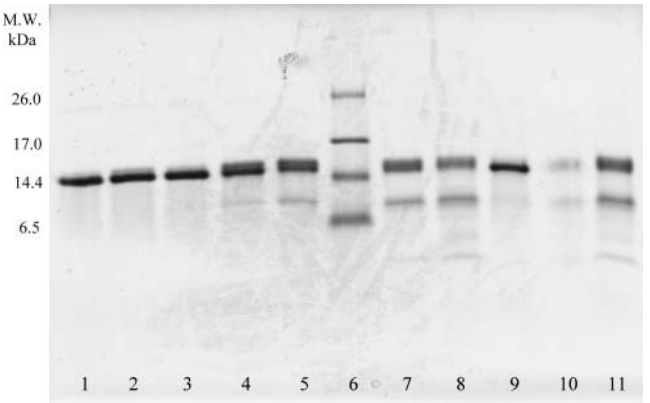

FIGURE 12 Tris-Tricine SDS-PAGE gel of different samples of HEWL. (*Lanes 1*, *2*, and *3*) Native HEWL at natural pH, pH 2.0, and pH 3.0, respectively. (*Lanes 4*, *5*, *7*, and *8*) HEWL at pH 2.0 heated for 24 h, 72 h, 168 h, and 11 days at 57°C. (*Lane 9*) pH 3.0, heated for 38 days. (*Lanes 10* and *11*) pH 2.0, heated for 11 days: in lane 10, filtered fraction of HEWL (only monomers), and in lane 11, only large aggregates. (*Lane 6*) Polypeptide molecular weight marker.

has to be at least partially destabilized to form fibrils (Dobson, 2001). Another common observation is that, at the same time, the protein molecule must be at least partially structured to form fibrils. In the work of Krebs et al. (2000) this is achieved by first heating the proteins at 100°C, freezing them in liquid nitrogen, followed by incubation at 37°C. We observe similar behavior using the much simpler procedure of incubation at a fixed temperature that was also used by Morozova-Roche et al. (2000) in their study of fibril formation of both native and mutated human lysozyme.

At pH 2.0, HEWL forms fibrils after incubation at temperatures between 57 and 80°C. At 57°C, close to the midpoint temperature of the unfolding transition, fibrils are formed after only ~2 days of incubation. At 80°C, we observe fibrils but also a lot of spherical aggregates. This is probably due to the fact that at this temperature, the protein molecule is already almost completely unfolded. Although the spherical aggregates are not the focus of this study, we should mention that sometimes proteins that form amyloid aggregates in vitro also form granular aggregates at specific conditions. For the case of the SH3 domain from bovine phosphatidyl-inositol-3′-kinase (PI-SH3) and the N-terminal domain of the *Escherichia coli* HypF protein (HypF-N) Bucciantini et al. (2002) have shown that not only fibrillar aggregates but also granular aggregates can be cytotoxic.

At pH 3.0 the protein is much more stable, and fibril formation only occurs after heating at 57°C for 11 days. Finally, at pH 4.0 we could not observe fibrils even after 42 days of incubation at 57°C because the protein is practically native at these conditions. Incubation at 80°C, pH 4.0, produced only small spherical aggregates. Spherical or granular aggregates are in some cases considered as precursors or nuclei for a fibril formation as in the case of amyloid β-protein studied by Lomakin et al. (1997). This is obviously not the case for HEWL aggregation in the pH range studied by us. At pH 2.0 we observe spherical aggregates together with fibrils mostly in samples heated at 80°C (Fig. 3 *a*). In samples heated at 57°C and at pH 2.0 we rarely observe spherical aggregates. Upon heating of HEWL solutions at pH 3.0 at 57°C we do not observe any spherical aggregates. If spherical aggregates were precursors or nuclei for fibril formation one would expect to observe them before fibril formation or together with the fibrils. As one can see in Fig. 3, *a–d*, the spherical aggregates observed by us are larger in diameter than the fibrils so they cannot be a precursor to the fibril formation.

Unfolding properties of the more unstable lysozyme at pH 2.0 seem to be unique in promoting the fibrillar aggregation of HEWL: simply heating to a temperature close to the midpoint of the unfolding transition, as we did for pH 4.0, is not enough. It is not just the distances to the midpoint of the unfolding transition that determines whether fibrils are formed or not. Evidently, HEWL unfolding pathways are different at pH 2.0 and pH 4.0, and fibril formation sensitively depends on these pathways. Unfolding pathways will also be different for unfolding induced by other means, such as by adding denaturants. The mechanism of fibril formation may therefore also be different for those cases. On the other hand, since there is such a wide range of solution conditions that give rise to fibril formation, for such a wide range of proteins, it is not unreasonable to expect that there are at least some mechanistic similarities, and that ultimately studies on model systems such as ours may contribute to a better understanding of fibril formation, e.g., in mutated human lysozyme.

In our SLS experiments, we observe that there is always a very distinct lag time before fibril formation starts. We have found that even when heating at 80°C, fibrils are observed by AFM only after 2 days, whereas spherical aggregates start forming immediately, as detected by light scattering and confirmed by AFM. If we assume that the lag time is due to some nucleation event, the concentration dependence of the lag time should reflect the number of protein monomers involved in nucleation. Although we are somewhat hampered by the fact that there is such a large spread in the lag time for individual samples, the averaged data suggest that there is in fact no significant dependence of lag time on concentration. This would imply that the nucleation event is in fact a monomolecular event, e.g., a slow transition of individual lysozyme molecules to a partially folded state that initiates fibril formation.

Since the lysozyme stability plays a crucial role in the fibril formation, we studied it with respect to temperature at different pH values, as well as the effect of the heating time on the protein structure at pH 2.0 and at 57°C. The stability of HEWL has been extensively studied (Redfield and Dobson, 1988; Radford et al., 1992; Itzhaki et al., 1994; Dobson et al., 1994; Yang et al., 1994; Hoshino et al., 1997; Kamatari et al., 1998; Yonezawa et al., 2002). Most of the studies, however, are concerned with the effect of alcohols on the structure and stability of the HEWL molecule, and not with the effect of temperature on the protein structure in water solutions. According to Kamatari et al. (1998), methanol induces an expanded helical conformation in HEWL. Similar effects were observed by Hoshino et al. (1997) in trifluoroethanol, where a highly cooperative transition to an open helical conformation was observed. Yang et al. (1994) studied a synthetic peptide corresponding to the antiparallel triple-stranded β-sheet in HEWL by CD and size-exclusion chromatography. They found that upon heating the polypeptide at pH 2.0 all the structure was lost at 65°C. The addition of trifluoroethanol, however, led to the formation of α-helical structure. Judging from CD data, Yonezawa et al. (2002) argue that the secondary structure of HEWL depends strongly on the protein concentration and on the presence of ethanol. For low protein concentration (2 mg/ml), the structure of HEWL is predominantly helical up to 80% ethanol, whereas for higher protein concentration (5 mg/ml), the structure is predominantly β-sheet above 75% ethanol.

Our studies of the structure of HEWL as a function of temperature and pH showed the following. The presence of single isodichroic points in Fig. 8, *a–c*, suggests that at all pH values studied by us the change in the secondary structure of the molecule, with respect to increasing temperature, is a two-state cooperative process (Fändrich et al. 2003). Our CD data also show (see Fig. 10 *a*) that when the temperature is kept close to the midpoint of the unfolding transition, after a rapid initial change, the spectrum keeps changing more slowly, toward increasing α-helix content, suggesting slow and continuous changes in the secondary structure of the partially folded HEWL molecules.

The jump observed in the molecular residue ellipticity at 222 nm (Fig. 10 *b*) shows that the change in the lysozyme structure as a function of the heating time occurs simultaneously for a large part of the protein molecules. The jump occurs within the time at which the fibril formation starts (see Light scattering). Another interpretation could be that the change in the secondary structure is due not to a slow collective transition of the protein molecules but to a very slowly increasing number of unfolded molecules due to the lower probability of the unfolding at a lower temperature.

Though some fibrils may inevitably form in the sample studied by CD upon prolonged heating, their concentration is not high enough to significantly influence the CD spectra. Results obtained from dilute solutions during continuous heating and results from concentrated solutions quenched and diluted after prolonged heating may differ, since the latter contain many more fibrils. That is why we also carried out experiments with HEWL samples quenched and diluted after certain heating times. Our results in Fig. 11 show that after 11 days of heating of HEWL at pH 2.0 at 57°C, the structure of the free monomers, as well as that of the monomers incorporated in the fibrils, differs a lot from the structure observed in Fig. 10 *a* and is predominantly a random coil. The minimum at 218 nm observed in the spectrum of the separated fibrils (*OLA*) could be caused by formation of intermolecular β-sheets by the protein molecules in the fibrils.

The kinetic data from the light scattering suggest that the fibril formation is not a cooperative multimolecular process, but rather a monomolecular one. The rate of fibril elongation should hold further mechanistic information. Fitting a kinetic model to the experimental data could help to resolve the type of the nucleation event, if present, and the type of the kinetic reaction (Ferrone, 1999; Hofrichter, 1986). Unfortunately, the rate of increase of the light scattering intensity (after the lag time) shows such a large spread that at present we cannot extract any reliable information on the rate of fibril elongation. Further analysis of the light scattering data is also complicated because the fibrils are strongly interacting and start overlapping already when very small amounts of fibrils have been formed.

The morphology of the fibrils formed from HEWL at different conditions varies from short and flexible (Goda et al., 2000) to long and stiff (Krebs et al., 2000; Cao et al., 2004). Cao et al. (2004) report 2–5 nm thickness and 1- to 2-μm length. The fibrils observed by Goda et al. (2000) are much shorter, 100–200 nm, and a bit thicker, ~7 nm. A thickness of ~7 nm is also reported by Krebs et al. (2000) with fibrils longer than 1 μm. We studied the morphology of the fibrils formed upon heating of HEWL water solutions at pH 2.0 and 3.0 at 57°C in great detail by AFM. For samples at pH 2.0 heated at 57°C we observe two populations of fibrils—thin, 2.5 $\pm$ 0.3 nm, and thick, 4.0 $\pm$ 0.7 nm (see Fig. 3, *c* and *d*, and Fig. 5 *a*). Similar sizes have been observed by Cao et al. (2004). The experimental data about the fine structure of the fibrils observed with the help of super-sharp AFM tips (Fig. 6) allows us to speculate about the origin of the fibril morphology. The thick fibrils seem to have a coiled structure with a period of ~30 nm. The two populations of the rodlike subunit (Fig. 4, *a* and *b*, and Fig. 5 *b*) with lengths of 124 $\pm$ 9 nm and 157 $\pm$ 11 could be due to a tension developing in the coil resulting in a defect every four or five turns. The thin fibrils most probably result from a straight association of protein molecules without any twist because the rodlike subunit is not observed in that case.

The fibrils obtained upon heating of HEWL at pH 3.0 at 57°C are also very long (of the order of 5 μm), with a similar thickness to those obtained at pH 2.0. They seem slightly more flexible and the rodlike unit is not observed.

Although protein hydrolysis does take place at pH 2.0, we do not think that it is crucial in the aggregation process. Malisauskas et al. (2003) arrived at a similar conclusion for the case of equine lysozyme. The arguments are that, first of all, at pH 3.0 there is no hydrolysis, but judging from light scattering and AFM experimental data, fibril formation is observed to be very similar to that at pH 2.0, albeit much slower, since HEWL is much more stable at pH 3.0. Second, if fragments play a special role in the aggregation process, one might expect that they would be preferentially incorporated into the fibrils. However, separated fibrils and (partly hydrolyzed) monomers are nearly identical in SDS-PAGE, suggesting an even distribution of fragments.

Now we can draw some parallels between fibrils formed from β-lg and HEWL. In both cases fibrils are formed at low ionic strength far from the isoelectric point of the protein. On the other hand the mechanism of fibril formation seems to depend strongly on the unfolding pathway of the protein at the particular conditions. In the case of β-lg the aggregation starts immediately when the heating is started (Arnaudov et al., 2003). This means that the structure of the β-lg molecule at 80°C, pH 2.0, is appropriate for fibril formation. Whether that is due to the large β-sheet content in the secondary structure of β-lg is a matter for further study. In the case of HEWL, simply increasing the temperature above the melting transition of the protein is not sufficient for fibril formation. The difference in the behavior of HEWL at pH 2.0, 3.0, and 4.0 can hardly be due to electrostatics because at all these pH values the protein molecule is strongly

charged (between 11 and 17 positive charges for the pH range between 4.0 and 2.0, respectively; Kuehner et al., 1999). The difference must be sought in the different unfolding pathways at different conditions. Even at pH 2.0, 2 days are needed for the HEWL molecules to adopt a configuration suitable for forming fibrils. Therefore, despite the similarities between the fibrillar structures formed from different proteins and the similarities between the conditions at which they form, a detailed approach is needed to establish the mechanism of fibril formation for every individual protein.

CONCLUSIONS

The stability of HEWL toward heat treatment is greatly influenced by the pH. The lower the pH, the lower the stability of the protein. The conditions at pH 2.0 are unique in promoting the fibrillar aggregation of HEWL since heating of solutions at pH 3.0 and 4.0 to temperatures just above the midpoint of the unfolding transition of the molecule does not lead to the appearance of fibrillar aggregates.

HEWL fibrils are formed after a lag time that is practically concentration-independent. This means that the governing process for the fibril formation is the change in the structure of single protein molecules caused by a prolonged exposure to a temperature close to the midpoint of the unfolding transition.

The fibril morphology is complex. The fibrils formed at pH 2.0 are long and straight with a length of the order of 5 μm and predominant thickness of $\sim$4 nm and consist of stiff rodlike subunits with length either 124 or 157 nm. On a smaller scale the fibrils consist of a coiled structure with a period of $\sim$30 nm that gives the appearance of the rodlike subunits probably because of defects occurring every four or five turns.

The fibrils consist mostly of full-length HEWL, although, some fragments due to hydrolysis at pH 2.0 and 57°C are probably incorporated into the fibrils. At any rate the hydrolysis of the protein is not the cause of the aggregation since at pH 3.0 no hydrolysis is detected but fibrils do form.

REFERENCES

Arnaudov, L. N., R. de Vries, H. Ippel, and C. P. M. van Mierlo. 2003. Multiple steps during the formation of β-lactoglobulin fibrils. *Biomacromolecules*. 4:1614–1622.

Aymard, P., T. Nicolai, and D. Durand. 1999. Static and dynamic scattering of β-lactoglobulin aggregates formed after heat-induced denaturation at pH 2. *Macromolecules*. 32:2542–2552.

Booth, D. R., M. Sunde, V. Bellotti, C. V. Robinson, W. L. Hutchinson, P. E. Fraser, P. N. Hawkins, C. M. Dobson, S. E. Radford, C. C. F. Blake, and M. B. Pepys. 1997. Instability, unfolding and aggregation of human lysozyme variants underlying amyloid fibrillogenesis. *Nature*. 385:787–793.

Bucciantini, M., E. Giannoni, F. Chiti, F. Baroni, L. Formigli, J. Zurdo, N. Taddel, G. Ramponi, C. M. Dobson, and M. Stefani. 2002. Inherent toxicity of aggregates implies a common mechanism for protein misfolding diseases. *Nature*. 416:507–511.

Cao, A., D. Hu, and L. Lai. 2004. Formation of amyloid fibrils from fully reduced hen egg white lysozyme. *Protein Sci*. 13:319–324.

Chamberlain, A. K., C. E. MacPhee, J. Zurdo, L. A. Morozova-Roche, H. A. O. Hill, C. M. Dobson, and J. J. Davis. 2000. Ultrastructural organization of amyloid fibrils by atomic force microscopy. *Biophys. J*. 79:3282–3293.

Dobson, C. M. 2001. The structural basis of protein folding and its links with human disease. *Philos. Trans. R. Soc. Lond. B*. 356:133–145.

Dobson, C. M., P. A. Evans, and S. E. Radford. 1994. Understanding how proteins fold: the lysozyme story so far. *Trends Biochem. Sci*. 19:31–37.

Fändrich, M., V. Forge, K. Buder, M. Kittler, C. M. Dobson, and S. Diekmann. 2003. Myoglobin forms amyloid fibrils by association of unfolded polypeptide segments. *Proc. Natl. Acad. Sci. USA*. 100:15463–15468.

Ferrone, F. 1999. Analysis of protein aggregation kinetics. *Methods Enzymol*. 309:256–274.

Goda, S., K. Takano, Y. Yamagata, R. Nagata, H. Akutsu, S. Maki, K. Namba, and K. Yutani. 2000. Amyloid protofilament formation of hen egg lysozyme in highly concentrated ethanol solution. *Protein Sci*. 9: 369–375.

Gosal, W. S., A. H. Clark, P. D. A. Pudney, and S. B. Ross-Murphy. 2002. Novel amyloid fibrillar networks derived from a globular protein: beta-lactoglobulin. *Langmuir*. 18:7174–7181.

Hofrichter, J. 1986. Kinetics of sickle hemoglobin polymerization III. Nucleation rates determined from stochastic fluctuations in polymerization progress curves. *J. Mol. Biol*. 189:553–571.

Hoshino, M., Y. Hagohara, D. Hamada, M. Kataoka, and Y. Goto. 1997. Trifluoroethanol-induced conformational transition of hen egg-white lysozyme studied by small-angle X-ray scattering. *FEBS Lett*. 416: 72–76.

Ikeda, S., and V. J. Morris. 2002. Fine-stranded and particulate aggregates of heat-denatured whey proteins visualized by atomic force microscopy. *Biomacromolecules*. 3:382–389.

Itzhaki, L. S., P. A. Evans, C. M. Dobson, and S. E. Radford. 1994. Tertiary interactions in the folding pathway of hen lysozyme: kinetic studies using fluorescent probes. *Biochemistry*. 33:5212–5222.

Jimenez, J. L., E. J. Nettleton, M. Bouchard, C. V. Robinson, C. M. Dobson, and H. R. Saibil. 2002. The protofilament structure of insulin amyloid fibrils. *Proc. Natl. Acad. Sci. USA*. 99:9169–9201.

Jimenez, J. L., G. Tennent, M. Pepys, and H. R. Saibil. 2001. Structural diversity of *ex vivo* amyloid fibrils studied by cryo-electron microscopy. *J. Mol. Biol*. 311:241–247.

Kamatari, Y. O., T. Konno, M. Kataoka, and K. Akasaka. 1998. The methanol-induceed transition and the expanded helical conformation in hen lysozyme. *Protein Sci*. 7:681–688.

Kavanagh, G. M., A. H. Clark, and S. B. Ross-Murphy. 2000. Heat-induced gelation of globular proteins: part 3. Molecular studies on low pH β-lactoglobulin gels. *Int. J. Biol. Macromol*. 28:41–50.

Koike, A., N. Nemoto, and E. Doi. 1996. Structure and dynamics of ovalbumin gels: 1. Gel induced by high-temperature heat treatment. *Polymer*. 37:587–593.

Krebs, M. R. H., D. K. Wilkins, E. W. Chung, M. C. Pitkeathly, A. K. Chamberlain, J. Zurdo, C. V. Robinson, and C. M. Dobson. 2000. Formation and seeding of amyloid fibrils from wild-type hen lysozyme and a peptide fragment from the β-domain. *J. Mol. Biol*. 300:541–549.

Kuehner, D. E., J. Engmann, F. Fergg, M. Wernick, H. W. Blanch, and J. M. Prausnitz. 1999. Lysozyme net charge and ion binding in concentrated aqueous electrolyte solutions. *J. Phys. Chem. B*. 103:1368–1374.

Langton, M., and A.-M. Hermansson. 1992. Fine-stranded and particulate gels of β-lactoglobulin and whey protein at varying pH. *Food Hydrocolloids*. 5:523–539.

Lomakin, A., D. B. Teplov, D. A. Kirschner, and G. B. Benedek. 1997. Kinetic theory of fibrillogenesis of amyloid β-protein. *Proc. Natl. Acad. Sci. USA*. 94:7942–7947.

Malisauskas, M., V. Zamotin, J. Jass, W. Noppe, C. M. Dobson, and L. A. Morozova-Roche. 2003. Amyloid protofilaments from the calcium-binding protein equine lysozyme: formation of ring and linear structures depends on pH and metal ion concentration. *J. Mol. Biol.* 330:879–890.

Morozova-Roche, L. A., J. Zurdo, A. Spencer, W. Noppe, V. Receveur, D. B. Archer, M. Joniau, and C. M. Dobson. 2000. Amyloid fibril formation and seeding by wild-type human lysozyme and its disease-related mutational variants. *J. Struct. Biol.* 130:339–351.

Nemoto, N., A. Koike, K. Osaki, T. Koseki, and E. Doi. 1993. Dynamic light scattering of aqueous solutions of linear aggregates induced by thermal denaturation of ovalbumin. *Biopolymers.* 33:551–559.

Pepys, M. B., P. N. Hawkins, D. R. Booth, D. M. Vigushin, G. A. Tennent, A. K. Soutar, N. Totty, G. Nguyen, C. C. F. Blake, C. J. Terry, T. G. Feest, A. M. Zalin, and J. J. Hsuan. 1993. Human lysozyme gene mutations cause hereditary systemic amyloidoses. *Nature.* 362:553–557.

Radford, S. E., C. M. Dobson, and P. A. Evans. 1992. The folding of hen lysozyme involves partially structured intermediates and multiple pathways. *Nature.* 358:302–307.

Redfield, C., and C. M. Dobson. 1988. Sequential ^{1}H NMR assignment and secondary structure of hen egg white lysozyme in solution. *Biochemistry.* 27:122–136.

Sagis, L. M. C., C. Veerman, and E. van der Linden. 2004. Mesoscopic properties of semiflexible amyloid fibrils. *Langmuir.* 20:924–927.

Sasahara, K., M. Demura, and K. Nitta. 2000. Partially unfolded state of hen lysozyme studied by circular dichroism spectroscopy. *Biochemistry.* 39:6475–6482.

Sunde, M., and C. C. F. Blake. 1998. From the globular to the fibrous state: protein structure and structural conversion in amyloid formation. *Q. Rev. Biophys.* 31:1–39.

Tanaka, S., Y. Oda, M. Ataka, K. Onuma, S. Fujiwara, and Y. Yonezawa. 2001. Denaturation and aggregation of hen egg lysozyme in aqueous ethanol solution studied by dynamic light scattering. *Biopolymers.* 59: 370–379.

Tani, F., M. Murata, T. Higasa, M. Goto, N. Kitabatake, and E. Doi. 1995. Molten globule state of protein molecules in heat-induced transparent food gels. *J. Agric. Food Chem.* 43:2325–2331.

Yang, J. J., M. Pitkeathly, and S. E. Radford. 1994. Far-UV circular dichroism reveals a conformational switch in a peptide fragment from the β-sheet of hen lysozyme. *Biochemistry.* 33:7345–7353.

Yonezawa, Y., S. Tanaka, T. Kubota, K. Wakabayashi, K. Yutani, and S. Fujiwara. 2002. An insight into the pathway of the amyloid fibril formation of hen egg white lysozyme obtained from a small-angle X-ray and neutron scattering study. *J. Mol. Biol.* 323:237–251.

Zurdo, J., I. Guijarro, and C. M. Dobson. 2001. Preparation and characterization of purified amyloid fibrils. *J. Am. Chem. Soc.* 123: 8141–8142.